



Effect of temperature on the pathogenesis, accumulation of viral and satellite RNAs and on plant proteome in peanut stunt virus and satellite RNA-infected plants

Aleksandra Obrepalska-Stęplowska^{1*}, Jenny Renaut², Sebastien Planchon², Arnika Przybylska¹, Przemysław Wieczorek¹, Jakub Barylski³ and Peter Palukaitis⁴

¹ Interdepartmental Laboratory of Molecular Biology, Institute of Plant Protection – National Research Institute, Poznań, Poland, ² Department Environmental Research and Innovation, Integrative Biology Facility, Luxembourg Institute of Science and Technology, Belvaux, Luxembourg, ³ Department of Molecular Virology, Adam Mickiewicz University, Poznań, Poland, ⁴ Department of Horticultural Sciences, Seoul Women University, Seoul, South Korea

OPEN ACCESS

Edited by:

Mark Findlay Belmonte,
University of Manitoba, Canada

Reviewed by:

Helene Sanfacon,
Agriculture and Agri-Food Canada,
Canada
Javier Plasencia,
Universidad Nacional Autónoma de
México, Mexico

*Correspondence:

Aleksandra Obrepalska-Stęplowska
olaob@o2.pl

Specialty section:

This article was submitted to
Plant Biotic Interactions,
a section of the journal
Frontiers in Plant Science

Received: 06 August 2015

Accepted: 09 October 2015

Published: 29 October 2015

Citation:

Obrepalska-Stęplowska A, Renaut J, Planchon S, Przybylska A, Wieczorek P, Barylski J and Palukaitis P (2015) Effect of temperature on the pathogenesis, accumulation of viral and satellite RNAs and on plant proteome in peanut stunt virus and satellite RNA-infected plants. *Front. Plant Sci.* 6:903. doi: 10.3389/fpls.2015.00903

Temperature is an important environmental factor influencing plant development in natural and diseased conditions. The growth rate of plants grown at 27°C is more rapid than for plants grown at 21°C. Thus, temperature affects the rate of pathogenesis progression in individual plants. We have analyzed the effect of temperature conditions (either 21°C or 27°C during the day) on the accumulation rate of the virus and satellite RNA (satRNA) in *Nicotiana benthamiana* plants infected by peanut stunt virus (PSV) with and without its satRNA, at four time points. In addition, we extracted proteins from PSV and PSV plus satRNA-infected plants harvested at 21 dpi, when disease symptoms began to appear on plants grown at 21°C and were well developed on those grown at 27°C, to assess the proteome profile in infected plants compared to mock-inoculated plants grown at these two temperatures, using 2D-gel electrophoresis and mass spectrometry approaches. The accumulation rate of the viral RNAs and satRNA was more rapid at 27°C at the beginning of the infection and then rapidly decreased in PSV-infected plants. At 21 dpi, PSV and satRNA accumulation was higher at 21°C and had a tendency to increase further. In all studied plants grown at 27°C, we observed a significant drop in the identified proteins participating in photosynthesis and carbohydrate metabolism at the proteome level, in comparison to plants maintained at 21°C. On the other hand, the proteins involved in protein metabolic processes were all more abundant in plants grown at 27°C. This was especially evident when PSV-infected plants were analyzed, where increase in abundance of proteins involved in protein synthesis, degradation, and folding was revealed. In mock-inoculated and PSV-infected plants we found an increase in abundance of the majority of stress-related differently-regulated proteins and those associated with protein metabolism. In contrast, in PSV plus satRNA-infected plants the shift in the temperature barely increased the level of stress-related proteins.

Keywords: plant-virus interactions, temperature change, plant proteomics, DIGE, cucumovirus, satellite RNA, leaf proteome, plant defense

INTRODUCTION

Temperature is one of the most important factors shaping the nature of plant pathogen interactions, as well as the normal development of healthy plants. Future changes in environmental conditions (Li et al., 2013), with an emphasis on the ambient temperature, will impact plants, plant pathogens, and consequently plant diseases (Suzuki et al., 2014; Ashoub et al., 2015). Environmental factors affect the growth, yield and populations of microorganisms living on plants, as well as vector populations, impacting the spread of plant pathogens. In the face of climate change it is of particular importance to investigate the plant performance comparisons at various temperature conditions, both when they are grown uninfected vs. challenged by various external biotic stimuli, including by important pathogens strictly dependent on the host cell life cycle, such as viruses. In the literature, there are contradictory data on the temperatures favoring viral replication, which depend on the tested virus species as well as the analyzed plant host. Higher temperatures resulted in more rigorous replication of turnip crinkle virus (TCV) in *Arabidopsis* plants (Zhang et al., 2012), and facilitated the spread of tobacco mosaic virus or turnip mosaic virus by weakening the plant defense responses (Király et al., 2008; Prasad and Sonnewald, 2013). On the other hand, plants infected by viruses and grown at higher temperature were less symptomatic due to more efficient RNA silencing-mediated plant defense (Szittyá et al., 2003; Chellappan et al., 2005; Tuttle et al., 2008). The importance of temperature on virus spread and plant defenses, including RNA silencing, is under intense investigation (Zhong et al., 2013; Ghoshal and Sanfaçon, 2014; Patil and Fauquet, 2015). Therefore, to assess how higher temperatures might alter plant-virus interactions, we analyzed the disease progress, viral and satellite RNA (satRNA) accumulation and characterization of plant proteome differences at two temperature conditions in the model plant *Nicotiana benthamiana*, using peanut stunt virus (PSV) and its satRNA.

PSV together with *Tomato aspermy virus* (TAV) and *Cucumber mosaic virus* (CMV) are all members of the genus *Cucumovirus* in the family *Bromoviridae*. Although the host range of PSV is more restricted than that of CMV, it occurs worldwide and infects a number of important crop species, as well as the model species *N. benthamiana*. PSV contains a positive-sense (+), single-stranded (ss) RNA genome and consists of three genomic and two subgenomic strands. RNA1 and RNA2 encode components of the viral replicase complex. RNA2 additionally encodes the 2b protein that is known to participate in viral movement and suppression of RNA silencing (Netsu et al., 2008). The 2b protein is synthesized from subgenomic RNA4A (Ding et al., 1994). RNA3 contains open reading frames for the movement protein (3a) and coat protein (CP; 3b). The latter is synthesized from subgenomic RNA4 (Schwinghamer and Symons, 1975). As with some CMV strains, some PSV strains may be associated with satRNA. One of the best known examples is the PSV-P strain (Pospieszny, 1987), later sequenced and classified in subgroup I of PSV (Obreńska-Stęplowska et al., 2008a,b). SatRNAs of PSV are linear, ssRNA molecules varying in length between 391 and 393 nt and do not encode

any functional proteins (Obreńska-Stęplowska et al., 2008a, 2012).

Infection by viruses may result in physiological changes in plants, manifested by macroscopically visible symptoms. At the molecular level, virus recognition by the host defense machinery results in the induction of plant defense responses, including those based on RNA silencing as well as others involving stress-response protein accumulation and their actions, to limit the invading pathogen accumulation (Lu et al., 2012; Pacheco et al., 2012; Zvereva and Pooggin, 2012; Obreńska-Stęplowska et al., 2013; Fang et al., 2015). The presence of satRNA adds further to this complexity modifying both symptom expression and plant responses. Some satRNAs associated with specific strains of cucumoviruses have been proposed to either interfere with the expression or function of viral RNA silencing suppressors (Hou et al., 2011; Shen et al., 2015), or compromise the induction or accumulation of other plant stress-related proteins (Hou et al., 2011; Obreńska-Stęplowska et al., 2013; Shen et al., 2015).

Since the levels of virus accumulation in plants are a product of actions undertaken by the host and the virus fitness under ambient conditions, we analyzed both the plant reaction at the proteome level and the levels of accumulation of virus genomic RNAs and satRNA in a susceptible host grown under both ambient and higher temperature conditions. Although the *N. benthamiana* transcriptome has been described (Nakasugi et al., 2013), many proteins are yet to be functionally characterized.

MATERIALS AND METHODS

Plants and Virus Materials

N. benthamiana plants were grown in strictly controlled conditions in separate breeding chambers with a 14 h light/10 h dark cycle, and after virus inoculations they were transferred to the appropriate temperature conditions: either 21°C day/16°C night, or 27°C day/24°C night. Infectious RNAs of PSV-P strain alone or in combination with satRNA-P (obtained as described in Obreńska-Stęplowska et al., 2013), were used for the inoculations to *N. benthamiana* plants at the four-leaf stage, in 0.05 M phosphate buffer, pH 7.5, after dusting the leaves with Carborundum. Mock-inoculated plants (treated only with inoculation buffer) were grown as negative control at both temperatures. The plants were harvested at 21 days post inoculation (dpi), when the first symptoms of infection developed in plants maintained at 21°C.

Comparative Assessment of the Accumulation of Viral and Satellite RNAs with Real-time PCR

A comparison of the accumulation of viral genomic RNA and a subgenomic RNA, as well as satRNA, in the infected plants was done using reverse-transcription (RT) real-time (quantitative) PCR (RT-qPCR) as described previously (Obreńska-Stęplowska et al., 2013). The RNA accumulation level was analyzed for each studied condition (mock-, PSV-, PSV and satRNA-inoculated plants) separately for five biological replicates. Each biological replicate was repeated thrice (technical replicates). The reaction

was done with primers pairs hybridizing to genes encoding each of the PSV open reading-frames (**Table 1**) in the Corbett Rotor-Gene 6000 (Qiagen) machine. For normalization, the level of the *N. benthamiana* β -actin gene transcription was used as a reference with primers NbActA/NbAct2 (Obrepałska-Stepłowska et al., 2013). An analysis and interpretation of the results was carried out using software integrated with the Corbett machine and REST 2009 Relative Expression Software Tool V2.0.13 (Qiagen) based on the $\Delta\Delta C_t$ method (Pfaffl et al., 2002).

Accumulation of Viral RNAs

Accumulation of PSV RNAs and satRNA was assessed by means of RT-qPCR. For this purpose whole plants infected with the virus were taken individually and were pulverized in liquid nitrogen using a mortar and pestle. A sample of the ground material was used for total RNA extraction using Trizol solution (Life Technologies). The RNA accumulation levels were analyzed for each studied condition separately for five biological replicates. Each biological replicate was repeated thrice (technical replicates). Aliquots of 0.5–1.0 μ g total RNA were first treated with RNase-free DNase and subsequently used for cDNA synthesis using Maxima H Minus First Strand cDNA Synthesis Kit supplemented with DNase (Life Technologies). The samples with 1.0 μ g of starting total RNA were diluted using an equal volume of water. Accumulation of RNA1, RNA3, and satRNA were done by RT-qPCR using the Power SYBR[®] Green PCR Master Mix (Applied Biosystems), the corresponding primers (**Table 1**) hybridizing to regions encoding for 1a, and CP proteins, or the satRNA, according to manufacturer's protocol. The reactions were performed with 9 μ l of master mix and 1 μ l of the cDNA (ca. 25 ng of used template RNA). For each set of primers a standard curve was prepared from a series of 10-fold dilutions of respective templates: for viral and satellite RNAs infectious clones of PSV were used (Obrepałska-Stepłowska et al., 2013). The relative distribution of the RNAs was normalized using *N. benthamiana* β -actin mRNA.

TABLE 1 | Primers used in reverse-transcription quantitative PCR analysis of the changes in the PSV and satellite RNA accumulation.

Primer name	Sequence	Region of amplification
PSVq1F	5' CTCTGCGCCTCGTTGATAAAG 3'	PSV ORF1a
PSVq1R	5' CATAACGATTTCAATCACTTC 3'	
PSVq2aF	5' CTCTTAGGTATCCCCGTAAG 3'	PSV ORF2a
PSVq2aR	5' CAAGCACATTGATACCCTATC 3'	
PSVq2bF	5' CTCmTATCCTCCAGCTA _y AC 3'	PSV ORF2b
PSVq2bR	5' GAATAACTCCCTCACACCAC 3'	
PSVq3aF	5' CTAGTCGGACTTTAACACAAC 3'	PSV ORF3a
PSVq3aR	5' ACGCTCATATATCCCTTAGAC 3'	
PSVqCPF	5' ACACATACACTTCGTTGGATG 3'	PSV ORFCP
PSVqCPR	5' CCTTCwTCTTCGGAAATTCAG 3'	
PARNA1	5' GGGAGGGCGGGCGTTCGTAGTG 3'	satRNA
PARNA2	5' GCCGTGGCCTTTCGTGGTC 3'	

Protein Extraction and Labeling

After 21 dpi, plants were harvested from each treatment (PSV-P, PSV-P/satRNA, and mock-inoculated plants, grown at both 21°C and 27°C). Four plants of similar growth were chosen for proteomic analyses. Fresh leaf materials (300 mg) from each plant were ground in liquid nitrogen and proteins were extracted and labeled as previously described (Obrepałska-Stepłowska et al., 2013). Samples containing 30 μ g of each Cy2 labeled internal standard, plus Cy3 and Cy5 labeled proteins for comparisons were pooled and lysis buffer (7M urea, 2M thiourea, 0.5% CHAPS) was added to a total volume of 120 μ l. Per the sampling conditions, four replicates were used (two labeled with Cy3 and two with Cy5). The samples representing biological replicates were tested separately.

2D-DIGE and Image Capture and Analysis

The following steps were done essentially as described previously (Obrepałska-Stepłowska et al., 2013). Briefly, 24 cm IPG strips, pH 3–10 NL (Bio-Rad) were rehydrated overnight with the 450 μ l of rehydration solution [the mixture of the Destreak rehydration solution (GE Healthcare) and Bio-lyte (Bio-Rad) per strip]. Proteins were cup-loaded on IPG strips and IEF was performed on an Ettan IPG-phor Manifold (GE Healthcare) with the following settings: initially, for 3 h at 150 V, then up to 1000 V over 5 h, a constant 1000 V for 4 h, then up to 10,000 V over 10 h and a final step at 10,000 V to reach 80,000 V-hr. Afterwards, strips containing proteins were equilibrated for 15 min in Equilibration buffer (Gel Company, San Francisco, CA) with an addition of 36% (w/v) urea and 1% (w/v) DTT. The strips then were equilibrated for another 15 min using the Equilibration buffer with 36% (w/v) urea and 2.5% (w/v) IAA, after which the strips were sealed with low-melt agarose (Gel Company) on top of the precast 12.5% acrylamide/bisacrylamide gels (Gel Company). Separation of proteins was done in an Ettan Dalt 12 apparatus (GE Healthcare) at 2.5 W/gel and at 15°C. After electrophoresis, gels with proteins labeled with Cy2, Cy3, and Cy5 were scanned with a Typhoon Variable Mode Imager 9400 (GE Healthcare). The collected images were analyzed using the Decyder v7.0 software (GE Healthcare). Spots were detected, and after matching and comparisons spot of interest, these were taken for mass spectrometry analysis.

Protein Identification

Picking, digestion with trypsin and spotting on MALDI targets were done as described by Renaut et al. (2006), with trypsin concentration of 8 μ g/ml. Then each sample (0.7 μ l) was deposited onto the target analyzed on a 4800 MALDI-TOF/TOF instrument (ABSciex, Foster City, CA, USA). Subsequently, searches were carried out using Mascot software in the NCBI "Viridiplantae" database (downloaded on 23 Sep 2013, 32770904 sequences), the "viruses" database (1220058 sequences), as well as EST for *Nicotiana* databases (downloaded on 2nd July 2014, 7936392 sequences). The search parameters allowed carboxyamidomethylation of cysteine (as fixed modification) and as oxidation of methionine and tryptophan and pyro-glu for N-term E or N-term Q (as variable modifications). A mass window of 100 ppm for peptide mass tolerance and 0.5 Da for

the fragment mass tolerance were allowed in searches. Homology identification was retained with a probability set at 95% and where needed, the identifications were verified manually.

Statistical Analysis

For a statistical analyses of the proteomic data, an ANOVA One-way and a *post-hoc* Student's *t*-test One-way ANOVA were applied and a significance level lower than $p < 0.05$ was taken into account. Statistically valid average changes >1.3 and <-1.3 between treatments were considered.

In silico Analysis of Protein Functions

Since annotation of many identified proteins and ESTs turned out to be incomplete we performed an array of complementary analyses to determine their functions. First, we applied Blast2GO software (Conesa and Götze, 2008) to associate GO terms with Mascot hits. This tool utilizes information on top BLAST hits (we performed local BLASTp or BLASTx search with *e*-value cut-off of $1e-25$ against set of all protein sequences of *Solanaceae* and *Arabidopsis thaliana* from RefSeq database) and predicted protein domains to annotate the query. Additionally we used KAAS (KEGG Automatic Annotation Server, Moriya et al., 2007) to acquire KEGG annotations. This tool classifies each sequence to an orthologous cluster and retrieves annotations assigned to it. Finally, we performed direct BLAST (Altschul et al., 1997) search against the tomato proteome (*Solanum lycopersicum*, up000004994) and manually gathered annotation from publicly available databases in order to compare identified proteins with sequences from well-annotated relatives. All obtained information were carefully curated and compared. KAAS identifications were used to project expression data onto KEGG metabolic networks of Tomato using CyKEGGParser (Cytoscape plugin developed by Nersisyan et al., 2014).

RESULTS

In this study, our aim was to assess changes occurring in plants that were grown at 27°C, when sister plants grown at 21°C started developing the first symptoms of virus expression, with regard to virus accumulation and specific plant responses. Additionally, prior to inoculation, all of the plants were grown at the same temperature (24°C) and were inoculated at a similar stage of growth. Some plants were inoculated with transcripts of genomic RNAs of PSV-P with or without satRNA, while others were inoculated with purified viral particles of wild-type PSV-P, naturally containing satRNA. In all cases, the symptoms were monitored. The first set of inoculated plants was used for proteomic analysis of the impact of the temperature on mock-inoculated, PSV-infected, and PSV plus satRNA-infected plants simultaneously, together with the relative comparison of viral and satRNA accumulation under these conditions. The second set of inoculated plants was used for the measurement of viral RNA and satRNA levels at various time points after inoculation.

Growth and Symptoms Appearance

Plants maintained under different temperature conditions grew at different rates. Faster growth and leaf development were

observed under the higher temperature conditions (27°C). Likewise, the progress of symptom development also was observed to be more rapid for plants kept at 27°C than at 21°C. In the former case, the onset of symptom development was observed about 14 dpi, while in the latter case about 21 dpi. Moreover, more rapid symptom development was observed in plants inoculated with purified viral particles vs. those plants inoculated with infectious genomic transcripts of PSV.

Comparison of Viral RNA and satRNA Levels in Plants Grown under Different Temperatures

A comparison was made of the accumulation levels of genomic and subgenomic RNAs of the virus with or without satRNA, at 21 dpi. In general, a decrease in accumulation of the analyzed RNAs was observed at higher temperature vs. the lower temperature (Figures 1A,B), with the exception of RNA4, the subgenomic RNA expressing the CP ORF, when plants were infected by PSV plus satRNA (Figure 1A). That the exception is in RNA4 accumulation rather than RNA3 and RNA4, was shown by the reduced accumulation of the RNA3, containing the 3a ORF (Figure 1A). Similarly, a four-fold drop in satRNA accumulation was observed in plants maintained at the higher temperature (Figure 1A).

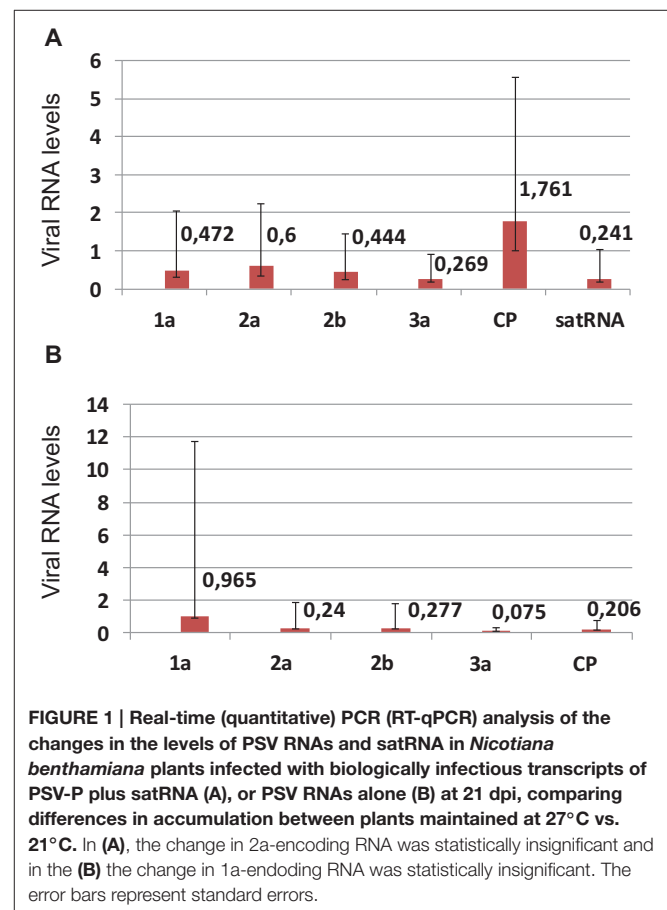


FIGURE 1 | Real-time (quantitative) PCR (RT-qPCR) analysis of the changes in the levels of PSV RNAs and satRNA in *Nicotiana benthamiana* plants infected with biologically infectious transcripts of PSV-P plus satRNA (A), or PSV RNAs alone (B) at 21 dpi, comparing differences in accumulation between plants maintained at 27°C vs. 21°C. In (A), the change in 2a-encoding RNA was statistically insignificant and in the (B) the change in 1a-encoding RNA was statistically insignificant. The error bars represent standard errors.

Accumulation of PSV RNA and satRNA during a Time Course of Infection at Two Temperatures

Since most of published data showed that viral RNA accumulation was greater at higher temperatures, (e.g., Király et al., 2008), we wanted to determine if plants infected with PSV and maintained at a higher temperature were accumulating viral RNAs less efficiently than those maintained at a lower temperature, or if PSV-infected plants reached a plateau of viral RNA accumulation earlier if grown at a higher temperature, followed by a drop in accumulation levels. In the latter case, this would suggest that at 21 dpi we were observing a reduced accumulation at the higher temperature while the plants grown at the lower temperature were showing a gradual increase. Thus, we conducted a time course of viral RNA accumulation over four time points in the infected plants, by RT-qPCR at the two temperatures, using primers specific to the RNAs containing ORF1 (RNA1) and ORF3b (CP; RNA3 and RNA4; **Figures 2A,B**) and to the satRNA (**Figure 2C**). The analyses showed that over 21 days of observation the accumulation levels of viral and satRNAs at the higher temperature increased rapidly after 11 dpi and then decreased between 15 and 21 dpi. On the other hand, in plants grown at the lower temperature, viral RNA accumulation increased gradually after 11 dpi, which then accelerated between 15 and 21 dpi. Thus, at 21 dpi the amounts of accumulated RNAs 1–3 and subgenomic RNA4, as well as satRNA, were all much lower at 27°C than at 21°C (**Figure 2**). The data show the accumulation profiles for viral genes and the satRNA. The differences in the scales may be due to primer performance. Importantly, the symptom expression associated with the high accumulation of virus started to develop just before 15 dpi in plants grown at 27°C and about 21 dpi in plants grown at 21°C (not shown).

Proteome Comparison of PSV Infected (with or without satRNA) and Mock-inoculated Plants Grown at Two Temperatures

To characterize the effect of plant maintenance at different temperatures on its proteome, *N. benthamiana* plants were grown over the same time period in separate greenhouse chambers with temperature sets at 21°C or 27°C during the day. When the first symptoms of infection were visible on the plants grown at 21°C, leaves of all plants were harvested. At this time point, plants grown at 27°C all had fully developed symptoms of disease and were significantly taller than those grown at 21°C. All plants were first tested for the presence or absence of PSV RNA and satRNA, as appropriate, and then used for proteomic profiling using DIGE analysis followed by Maldi TOF/TOF mass spectrometry and Mascot searches.

The plants were analyzed in three separate sets comparing the proteome analysis results for the two temperatures: (1) between mock-inoculated plants; (2) between plants infected by transcripts of the genomic PSV RNAs; and (3) between plants infected by both transcripts of the genomic PSV plus satRNA.

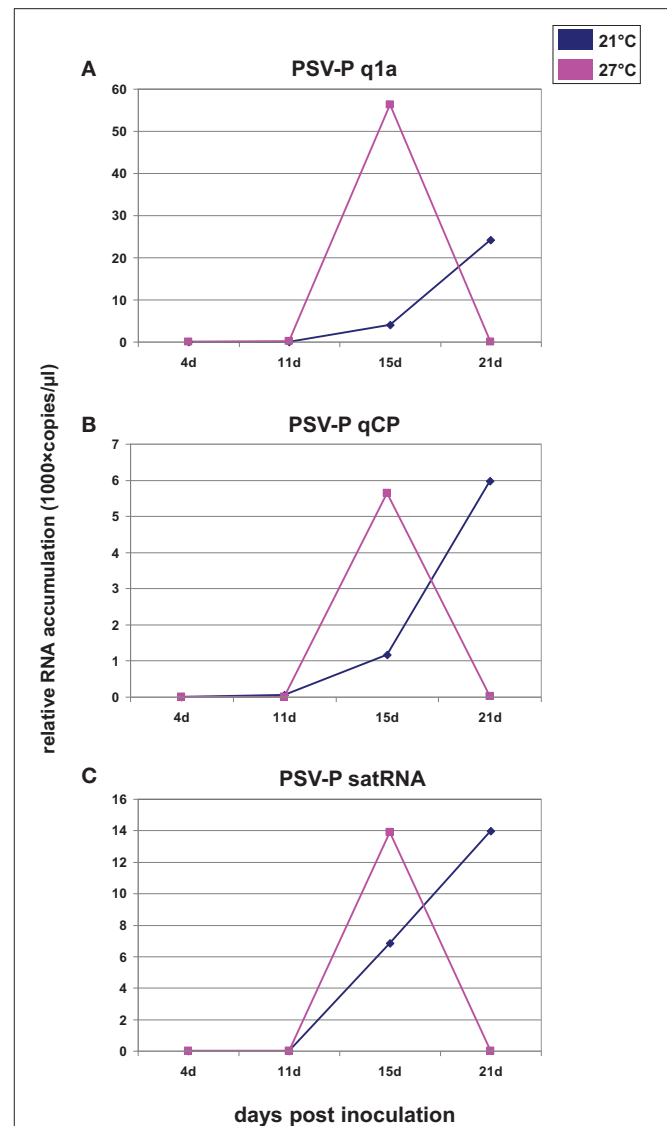


FIGURE 2 | Quantification of the number of copies of ORF1 (A), ORF3b (CP; B), and satRNA (C) assessed on the basis of accumulation of all relative to reference gene. The inoculum was wild-type PSV-P naturally containing satRNA. X axis shows the time points analyzed and Y axis shows the number of copies (in thousands) of analyzed RNAs. At 21 dpi, the level of ORF1a, CP, and satRNA tended toward zero. The experiment was repeated twice with similar results. The results derived from a single experiment are shown.

On the basis of DIGE analysis and MS/Mascot searches 38, 57, and 28 differentially-accumulated protein spots were found in mock-inoculated, PSV-infected, and PSV plus satRNA-infected plants, respectively, among which 23, 42, and 24, respectively, were identified and functionally annotated (**Tables 2–4**).

Influence of Temperature on Plant Proteome in Mock-inoculated Plants

In the case of mock-inoculated plants, most of the differentially-accumulated proteins were identified as being involved

TABLE 2 | Differentially-accumulated proteins in mock-inoculated *Nicotiana benthamiana*.

Control (mock-inoculated plants)					
Spot	Mascot hit	T-test	Av ratio*	Curated name	Other GOs
PHOTOSYNTHESIS AND CARBOHYDRATE METABOLIC PROCESS					
1412	gij77745458 gb ABB02628.1	0.0035	1.82	Triosephosphate isomerase	–
810	gij445628 prf 1909374A	0.024	1.62	Rubisco activase	Response to stimulus
1262	gij12643758 sp Q40565.1 RCA2_TOBAC	0.045	–1.39	Rubisco activase	Response to stimulus
963	gij362799991 dbj BAL41455.1	0.047	–1.41	Fructose 1,6, biphosphate aldolase	–
1319	gij62865755 gb AAY17070.1	0.025	–1.45	Carbonic anhydrase	–
768	gij159227386 emb CAJ80484.1	0.028	–1.62	ATP synthase CF1 beta subunit	–
1302	gij3914940 sp O20252.1 S17P_SPIOL	0.045	–1.94	Sedoheptulose-1,7-bisphosphatase, chloroplastic	–
1896	gij190146228 gb FG644758.1 FG644758	0.0077	–2	Photosystem II reaction center PSB28 protein	–
1295	gij62865755 gb AAY17070.1	0.038	–7.27	Carbonic anhydrase	–
CELLULAR AMINO ACID METABOLIC PROCESS					
770	gij12643806 sp Q9LEC8.1 DHEB_NICPL	0.014	–1.63	Glutamate dehydrogenase	Response to stimulus
PROTEIN METABOLIC PROCESS					
1540	gij357480975 ref XP_003610773.1	0.029	2.83	Proteasome subunit beta type-2-A-like	–
1407	gij14594931 emb CAC43326.1	0.044	2.46	Proteasome subunit beta type-5-like	–
1741	gij460407957 ref XP_004249415.1	0.048	1.86	Ubiquitin-conjugating enzyme E2 variant 1D	Response to stimulus
1814	gij508712318 gb EOY04215.1	0.0089	1.66	Ribosomal protein PSRP3/Ycf65	–
678	gij39857235 gb CK284052.1 CK284052	0.0034	1.52	Peptidase m20 m25 m40 family protein	–
RESPONSE TO STIMULUS					
1555	gij134642 sp P22302.1 SODF_NICPL	0.026	2.99	Superoxide dismutase [Fe]	–
1059	gij460385950 ref XP_004238663.1	0.0024	1.97	Quinone oxidoreductase-like protein	Photosynthesis
1601	gij543176812 gb AGV54429.1	0.014	1.8	Peroxiredoxin	Photosynthesis
1194	gij460397188 ref XP_004244150.1	0.035	–1.48	Thiamine thiazole synthase 1, chloroplastic-like	–
TRANSPORT					
405	gij350537279 ref NP_001234287.1	0.015	–1.69	Vacuolar H ⁺ -ATPase A2 subunit	–
406	gij350537279 ref NP_001234287.1	0.014	–1.8	Vacuolar H ⁺ -ATPase A2 subunit	–
408	gij350537279 ref NP_001234287.1	0.013	–1.86	Vacuolar H ⁺ -ATPase A2 subunit	–
NO ANNOTATION AVAILABLE					
1101	gij52580767 gb CV292958.1 CV292958	0.031	2.12	Oxidoreductase, zinc binding dehydrogenase family protein	–

Av. ratio = the average ratio derived from four measurements. Av. ratio cells are colored according to the value (red represents highest, green lowest and yellow intermediate ratios). T-test column is colored according to p-values (lowest values are green, higher ones are paler).

in photosynthesis and processes associated with general carbohydrate metabolism (11; seven decreased in abundance at the higher temperature), protein metabolic processes (five; all increased), or response to stimulus (eight; five increased) (Table 2). Also, a decrease was observed in the amounts of three protein spots for vacuolar H⁺-ATPase A2 subunit potentially involved in intra and intercellular transport (Table 2).

Influence of Temperature on the Plant Proteome in PSV-infected Plants

When plants infected with PSV were compared at two temperatures, the majority of the identified differentially-accumulated proteins were involved in carbohydrate metabolic processes including photosynthesis (Table 3). These were present in smaller quantities in comparison to plants grown at the lower temperature. Only one protein (involved in glycolysis) was more abundant. Similarly, as for mock-inoculated plants, the proteins involved in protein metabolic processes mostly increased in accumulation (11 of 14; Table 3). However, also

among the identified differentially-accumulated proteins are those participating in the processes of synthesis, assembly (including chaperones and chaperone-like) and degradation. Twenty differentially-accumulating protein spots were identified as involved in plant responses to stimulus. Among these, 12 proteins were more abundant and eight proteins were less abundant. Most proteins identified within this group could function in other processes, such as: five in photosynthesis (all less abundant); two for methionine synthase in cellular amino acid metabolic processes (both more abundant); and five in protein metabolic processes [ubiquitin-conjugating enzyme E2, heat shock 70 kDa protein (2 spots), chaperonin CPN60, and peptidyl-prolyl cis-trans isomerase; all more abundant at 27°C]. Three other proteins from the last category were less abundant, including spots containing hsp70 and peptidyl-prolyl cis-trans-isomerase. Several proteins in this group showed both an increase in abundance as well as a decrease in abundance, in different spots (Table 3). These include heat shock proteins and peptidyl-prolyl cis-trans isomerase. This might reflect the

TABLE 3 | Differentially-accumulated proteins in *Nicotiana benthamiana* infected by PSV.

Peanut stunt virus–infected plants					
Spot	Mascot hit	T-test	Av ratio	Curated name	Other GOs
PHOTOSYNTHESIS AND CARBOHYDRATE METABOLIC PROCESS					
1412	gj 77745458 gb ABB02628.1	0.0079	1.55	Triosephosphate isomerase	–
1908	gj 548526 sp P35477.1 PLAS2_TOBAC	0.038	–1.33	Plastocyanin	–
939	gj 460400830 ref XP_004245935.1	0.047	–1.53	Phosphoribulokinase, chloroplastic-like	–
1302	gj 3914940 sp O20252.1 S17P_SPIOL	0.043	–1.68	Sedoheptulose-1,7-bisphosphatase, chloroplastic	–
620	gj 460411525 ref XP_004251160.1	0.016	–1.69	Rubisco large subunit-binding protein subunit alpha (chaperonin 60 alpha)	Response to stimulus
1129	gj 460373374 ref XP_004232495.1	0.036	–1.81	Ferredoxin–NADP reductase, leaf isozyme, chloroplastic-like	Response to stimulus
1050	gj 356624532 pdb 3T15 A	0.027	–1.86	Rubisco activase	Response to stimulus
1490	gj 4930130 pdb 1RPX A	0.045	–2.06	Ribulose-phosphate 3-epimerase	–
1113	gj 350536711 ref NP_001234005.1	0.013	–2.16	Glyoxisomal malate dehydrogenase	–
686	gj 460401720 ref XP_004246365.1	0.045	–2.2	Fructose-1,6-bisphosphatase, chloroplastic-like	Photosynthesis
706	gj 460401720 ref XP_004246365.1	0.0079	–2.23	Fructose-1,6-bisphosphatase, chloroplastic-like	Photosynthesis
1294	gj 508726009 gb EOY17906.1	0.023	–2.23	Chloroplast sedoheptulose-1,7-bisphosphatase	Response to stimulus
1319	gj 62865755 gb AAAY17070.1	0.03	–2.38	Carbonic anhydrase	–
696	gj 7708648 emb CAB89998.1	0.0064	–2.41	ATP synthase CF1 beta subunit	–
802	gj 460370413 ref XP_004231047.1	0.024	–2.57	Glycerate dehydrogenase (hydroxypyruvate reductase), peroxisomal	–
874	gj 362799991 dbj BAL41455.1	0.013	–3.1	Fructose 1,6, bisphosphate aldolase	–
1084	gj 460373374 ref XP_004232495.1	0.0014	–3.61	Ferredoxin–NADP reductase, leaf isozyme, chloroplastic-like	Response to stimulus
1030	gj 255566555 ref XP_002524262.1	0.024	–3.98	Malate dehydrogenase	–
CELLULAR AMINO ACID METABOLIC PROCESS					
1425	gj 76870188 gb DV161180.1 DV161180	0.0085	2.59	Arginine biosynthesis bifunctional protein ArgJ	–
256	gj 8439545 gb AAF74983.1 AF082893_1	0.0034	2.07	Methionine synthase	Response to stimulus
237	gj 530704703 gb AGT40326.1	0.039	1.95	Methionine synthase	Response to stimulus
797	gj 190813280 gb FG200828.1 FG200828	0.016	–1.41	Aminomethyltransferase, mitochondrial (Glycine cleavage system T protein)	–
PROTEIN METABOLIC PROCESS					
1540	gj 357480975 ref XP_003610773.1	0.038	2.63	Proteasome subunit beta type-2-A-like	–
1867	gj 311124976 gb HS084903.1 HS084903	0.008	2.33	FKBP-type peptidyl-prolyl cis-trans isomerase	–
1828	gj 28261753 ref NP_783267.1	0.042	2.14	Ribosomal protein L14	–
477	gj 255554262 ref XP_002518171.1	0.0033	1.85	Chaperonin CPN60	Response to stimulus
1845	gj 94330105 gb EB683707.1 EB683707	0.0058	1.84	FKBP-type peptidyl-prolyl cis-trans isomerase	–
1655	gj 356536583 ref XP_003536816.1	0.0028	1.65	Peptidyl-prolyl cis-trans isomerase	Response to stimulus
1754	gj 460407957 ref XP_004249415.1	0.018	1.55	Ubiquitin-conjugating enzyme E2 variant 1D	Response to stimulus
678	gj 39857235 gb CK284052.1 CK284052	0.01	1.41	Peptidase m20 m25 m40 family protein	–
1096	gj 460407825 ref XP_004249350.1	0.047	1.37	Cochaperone GrpE family protein	–
620	gj 460411525 ref XP_004251160.1	0.016	–1.69	Rubisco large subunit-binding protein subunit alpha (chaperonin 60 alpha)	Response to stimulus
1657	gj 460365069 ref XP_004228428.1	0.015	–3.43	Peptidyl-prolyl cis-trans isomerase	Response to stimulus
RESPONSE TO STIMULUS					
388	gj 460369188 ref XP_004230445.1	0.0029	2.73	Heat shock 70 kda protein	Protein metabolic process, transport
1809	gj 134616 sp P27082.2 SODC_NICPL	0.031	1.94	Superoxide dismutase [Cu-Zn]	–
1204	gj 460373807 ref XP_004232705.1	0.03	1.75	Lactoylglutathione lyase-like (glyoxalase homolog)	–
424	gj 460369188 ref XP_004230445.1	0.028	1.66	Heat shock 70 kda protein	Protein metabolic process, transport
1236	gj 39859660 gb CK285269.1 CK285269	0.0023	1.63	NADH-cytochrome b5 reductase-like protein-like	–

(Continued)

TABLE 3 | Continued

Peanut stunt virus—infected plants					
Spot	Mascot hit	T-test	Av ratio	Curated name	Other GOs
852	gj 304368145 gb ADM26718.1	0.029	−2.22	Glycolate oxidase	–
328	gj 460369188 ref XP_004230445.1	0.01	−2.35	Heat shock 70 kda protein	Protein metabolic process, transport
RNA BINDING					
1119	gj 460391607 ref XP_004241412.1	0.038	1.69	Stem-loop (RNA) binding protein of 41 kda chloroplastic-like	Response to stimulus
1929	gj 47512378 gb CN747381.1 CN747381	0.018	1.56	Ribonucleoprotein	–
TRANSPORT					
1940	gj 254629991 gb FS376425.1 FS376425	0.022	1.72	Nuclear transport factor 2-like	Response to stimulus

Av. ratio cells are colored according to the value (red represents highest, green lowest and yellow intermediate ratios). T-test column is colored according to p-values (lowest values are green, higher ones are paler).

reaction of various forms or isoforms of these proteins to the applied conditions, as well as the fact that they have a role in both protein metabolism and plant responses to external stimulus. Interestingly, two proteins (spots no 1119 and 1929) involved in RNA interactions also were observed in higher amounts (Table 3); the first one might also participate in plant reactions to external stresses. This suggests there may be the intense re-organization within infected cells.

Influence of Temperature on the Plant Proteome in PSV-infected Plants in the Presence of satRNA

A comparison of plants grown under two temperature conditions and co-infected with PSV and its satRNA showed less abundant accumulation of proteins associated with photosynthesis and carbohydrate metabolism at higher temperature than was observed at the lower temperature (Table 4). There was a greater reduction in the amount of these proteins in PSV plus satRNA-infected plants, when compared to the plants infected with PSV alone, grown under the corresponding conditions. This decrease is especially evident for such proteins as ribulose biphosphate carboxylase/oxygenase (RuBisCo) small subunit, RuBisCo large subunit and carbonic anhydrase (Table 4). Plant defense was less pronounced and only seven protein spots classified as being involved in plant response to stimulus were identified, four decreasing in abundance at the higher temperature and three increasing (Table 4); only chaperonin 20, peptidyl-prolyl cis-trans isomerase (both in protein metabolic processes), and peroxiredoxin (associated with photosynthetic activities) were more abundant. One of two proteins identified as involved in nucleotide binding was more abundant, while the second was less abundant. The rest of the identified proteins associated with small molecule metabolic processes and transport were observed as less abundant at the higher temperature of growth (Table 4).

Comparison of all Treatment Conditions

To establish the general impact of the temperature on the plants grown under the different infection conditions, we compared all

the results to identify the proteins that in all treatments were either less abundant or more abundant (Table 5). In the present study, changes in the levels of proteins taking part in the Calvin cycle, tricarboxylic acid (TCA) cycle, glycolysis, as well as fructose and mannose metabolism were observed (Figure 3). Overall, a differential abundance of 11 protein spots in carbohydrate metabolism (including photosynthesis) was observed for mock-inoculated plants at the two temperature conditions, among which the levels of seven decreased at the higher temperature. In the case of spots for RuBisCo activase-containing sequences, both increased and decreased accumulation were found, which might be associated with its function in the maintenance of CO₂ fixation (Law and Crafts-Brandner, 2001) and in increasing the rate of photosynthesis during temperature changes (Yamori et al., 2012). In the case of virus-challenged plants, 18 protein spots involved in photosynthesis and carbohydrate metabolism differentially accumulated and 17 of these were in lesser amounts at the higher temperature; not only proteins involved in photosynthesis, but also proteins in the TCA cycle were found in smaller quantities during high temperature stress (Gammulla et al., 2011). Infection by PSV plus satRNA caused a decrease of 15 out of 16 differentially-accumulating proteins involved in photosynthesis and carbohydrate metabolism. This shows clearly that within the temperature range examined the increase in temperature caused a decrease in the level of proteins with a role in carbohydrate metabolism, which was particularly obvious in plants infected by PSV and PSV plus satRNA.

It is also interesting to note the changes in the proteins involved in protein and amino acid metabolism in plants maintained at the two temperatures. Mock-inoculated plants grown at the higher temperature all had five differentially-accumulated identified spots that were more abundant. However, four of them, were mostly involved in protein degradation (proteasome subunit beta type-2 and 5, ubiquitin-conjugating enzyme E2 and peptidase m20/m25/m40 family), and one protein was in the plastid ribosome function (ribosomal protein PSRP3). On the other hand, plants infected by PSV have 14 differentially-accumulated protein spots due to the change of temperature. Among

TABLE 4 | Differentially-accumulated proteins in *Nicotiana benthamiana* infected by PSV plus satRNA.

Peanut stunt virus plus satRNA-co-infected plants						
Spot	Mascot hit	T-test	Av ratio	Curated name	Other GOs	
PHOTOSYNTHESIS AND CARBOHYDRATE METABOLIC PROCESS						
338	gj 37359708 dbj BAC98299.1	0.045	-1.61	Beta-xylosidase alpha-l-arabinofuranosidase	-	
336	gj 37359708 dbj BAC98299.1	0.029	-1.49	Beta-xylosidase alpha-l-arabinofuranosidase	-	
365	gj 37359708 dbj BAC98299.1	0.0053	-1.49	Beta-xylosidase alpha-l-arabinofuranosidase	-	
363	gj 254658228 gb FS388360.1 FS388360	0.00049	-1.55	Beta-d-xylosidase 7-like	-	
1864	gj 3914596 sp Q39748.1 RBS6_FLAPR	0.018	-2.5	Ribulose-1,5-bisphosphate carboxylase, small subunit precursor	-	
1365	gj 22550386 gb AAL51055.2 AF454759_1	0.029	-2.72	Carbonic anhydrase	-	
1361	gj 62865755 gb AAY17070.1	0.042	-2.93	Carbonic anhydrase	-	
1877	gj 13241101 gb AAK16227.1 AF044395_1	0.049	-3.14	Ribulose-1,5-bisphosphate carboxylase small chain 3b	-	
1344	gj 115473 sp P27141.1 CAHC_TOBAC	0.026	-3.29	Carbonic anhydrase	-	
546	gj 1352794 sp P48709.1 RBL_NICDE	0.042	-3.57	Ribulose-1,5-bisphosphate carboxylase/oxygenase large subunit	-	
1303	gj 62865755 gb AAY17070.1	0.036	-4.24	Carbonic anhydrase	-	
1379	gj 62865755 gb AAY17070.1	0.042	-4.83	Carbonic anhydrase	-	
1868	gj 225905973 gb ACO35888.1	0.047	-4.96	Ribulose-1,5-bisphosphate carboxylase, small subunit	-	
1885	gj 47512534 gb CN747537.1 CN747537	0.0076	-7.04	Ribulose bisphosphate carboxylase small chain, chloroplastic	Response to stimulus	
1362	gj 62865755 gb AAY17070.1	0.036	-7.12	Carbonic anhydrase	-	
CELLULAR AMINO ACID METABOLIC PROCESS						
832	gj 40457328 gb AAR86719.1	0.045	-2.13	Glutamine synthetase	-	
PROTEIN METABOLIC PROCESS						
1489	gj 15242045 ref NP_197572.1	0.039	1.64	Chaperonin 20	Response to stimulus	
1655	gj 356536583 ref XP_003536816.1	0.015	1.59	Peptidyl-prolyl cis-trans isomerase	Response to stimulus	
RESPONSE TO STIMULUS						
1601	gj 543176812 gb AGV54429.1	0.028	1.52	Peroxiredoxin	Photosynthesis	
523	gj 117689576 gb DB688765.1 DB688765	0.019	-1.54	Glutathione reductase	-	
1752	gj 460365514 ref XP_004228646.1	0.044	-1.57	Zkt protein containing k-box and a tpr region	-	
RNA BINDING						
1910	gj 94326102 gb EB679704.1 EB679704	0.017	2.44	RNA recognition motif-containing protein	-	
1346	gj 133248 sp P19683.1 ROC4_NICSY	0.042	-1.82	31 kDa RNA binding protein	Response to stimulus	
TRANSPORT						
406	gj 350537279 ref NP_001234287.1	0.034	-1.5	Vacuolar H ⁺ -ATPase A2 subunit	-	

Av. ratio cells are colored according to the value (red represents highest, green lowest and yellow intermediate ratios). T-test column is colored according to p-values (lowest values are green, higher ones are paler).

these, 11 are more abundant at the higher temperature. These include proteins involved in processes of synthesis, degradation and transformation, including chaperones, likewise found previously (Gammulla et al., 2011). This indicates an intense effect on protein metabolism in virus-infected plants.

There are only a few differentially-accumulating proteins for which the fold-change for the two tested conditions is statistically significant (Table 5). Nevertheless, from this comparison it is evident that proteins involved in photosynthesis, carbohydrate metabolism and transport all decreased in accumulation, while proteins involved in plant defense and some aspects of protein metabolism increased in accumulation.

No statistically significant decrease or increase of abundance of either the pathogenesis responsive proteins, or proteins involved in RNA silencing was observed in all three comparisons, which might result from either there being no change in the levels

of these proteins under the studied conditions, or these proteins levels being below the limit of detection.

Annotation and Visualization of the Expression Data

Blast2GO assigned provisional names and GO terms to 83 (100%) of the Mascot hits. Direct BLAST search against the tomato proteome revealed 69 putative homologs and allowed us to annotate 36 of them with at least one KEGG term. The KAAS server, on the other hand, mapped only 57 proteins to 40 orthologous clusters (which suggests a degree of redundancy in the analyzed set), but assigned 37 of them to KEGG pathways. Results of the final curation and data comparison are presented in **Supplementary Table S1**, while proposed functional classification is shown in **Tables 2–4**. Only a part of the differently expressed proteins could be successfully mapped on Tomato KEGG pathways. While some of them could

TABLE 5 | Data summary of proteins that are more abundant (green) or less abundant (pink) at higher temperature under all conditions.

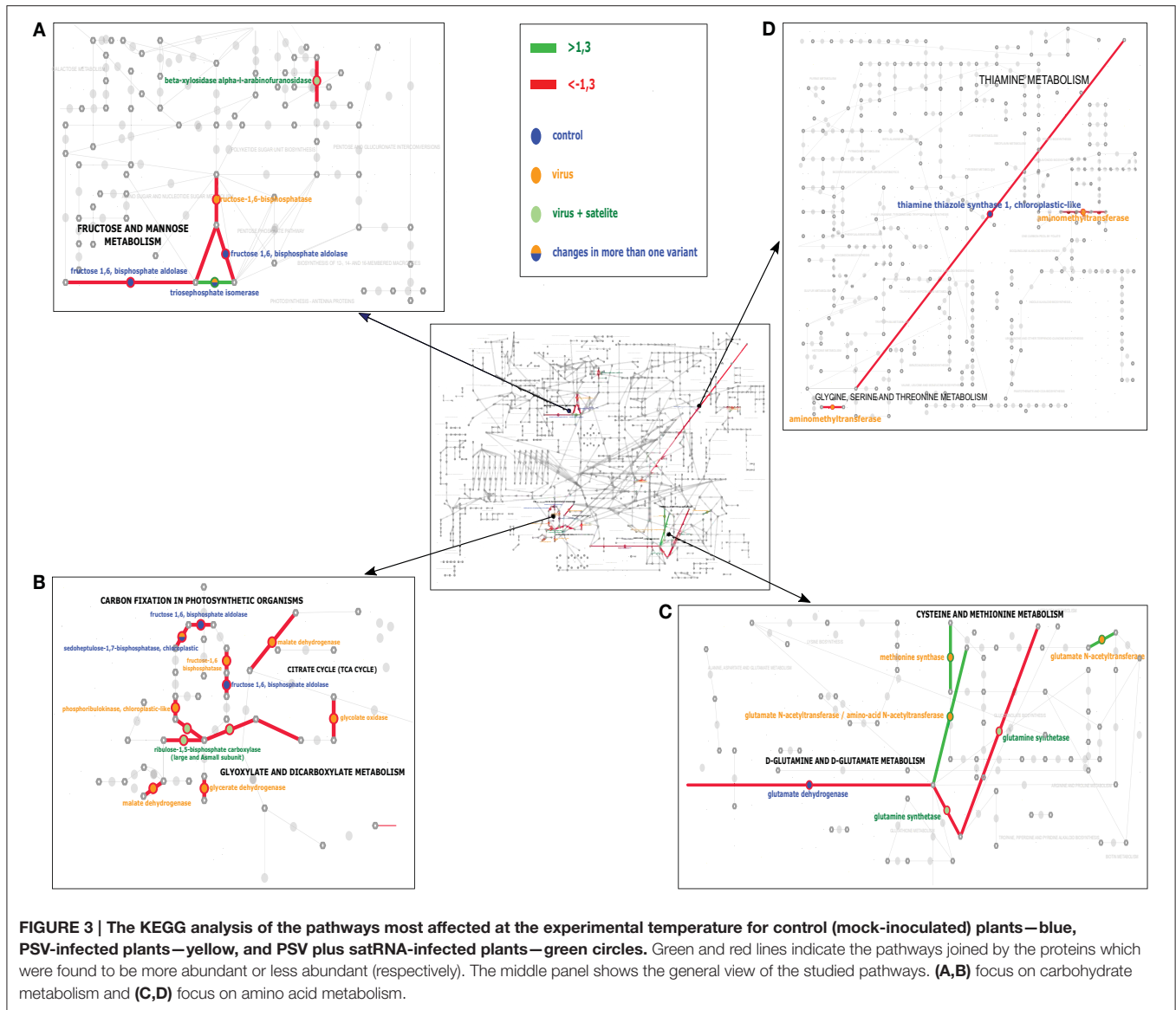
No.	Curated name	Av. Ratio (mock-inoculation)	Av. Ratio (PSV-inoculation)	Av. Ratio(PSV + satRNA-inoculation)	Processes
363	Beta-d-xylosidase 7-like	-1.74	-1.24	-1.55	Photosynthesis and carbohydrate metabolism
377	Malate dehydrogenase	-1.61	-1.61	-1.42	Photosynthesis and carbohydrate metabolism
696	ATP synthase beta subunit	-1.46	-2.41	-1.46	Photosynthesis and carbohydrate metabolism
874	Fructose-bisphosphate aldolase	-1.58	-3.1	-1.9	Photosynthesis and carbohydrate metabolism
1294	Sedoheptulose-1; 7-bisphosphatase	-2.09	-2.23	-2.15	Photosynthesis carbohydrate metabolism/ response to stimulus
1295	Carbonic anhydrase	-7.27	-5.38	-1.56	Photosynthesis and carbohydrate metabolism
1302	Sedoheptulose-1; 7-bisphosphatase; chloroplastic	-1.94	-1.68	-2.28	Photosynthesis and carbohydrate metabolism
1303	Carbonic anhydrase	-3.06	-7.05	-4.24	Photosynthesis and carbohydrate metabolism
1344	Carbonic anhydrase	-2.1	-3	-3.29	Photosynthesis and carbohydrate metabolism
1361	Carbonic anhydrase	-2.19	-3.42	-2.93	Photosynthesis and carbohydrate metabolism
1362	Carbonic anhydrase	-3.95	-15.34	-7.12	Photosynthesis and carbohydrate metabolism
1365	Carbonic anhydrase	-2.56	-4.19	-2.72	Photosynthesis and carbohydrate metabolism
1379	Carbonic anhydrase	-2.8	-14.32	-4.83	Photosynthesis and carbohydrate metabolism
1657	Peptidyl-prolyl cis-trans isomerase	-1.57	-3.43	-1.52	Protein metabolism/response to stimuli
1686	23 kDa polypeptide of photosystem II oxygen-evolving complex	-1.84	-1.47	-1.48	Photosynthesis
1896	Photosystem II reaction center PSB28 protein	-2	-1.32	-1.42	Photosynthesis and carbohydrate metabolism
1885	Ribulose biphosphate carboxylase small chain, chloroplastic	-1.25	-2.05	-7.04	Photosynthesis and carbohydrate metabolism/response to stimuli
523	Glutathione reductase	-1.35	-1.84	-1.54	Response to stimuli
405	Vacuolar H ⁺ -ATPase A2 subunit	-1.69	-1.37	-1.58	Transport
406	Vacuolar H ⁺ -ATPase A2 subunit	-1.8	-1.38	-1.5	Transport
408	Vacuolar H ⁺ -ATPase A2 subunit	-1.86	-1.27	-1.37	Transport
1059	Quinone oxidoreductase-like protein	1.97	1.24	1.21	Response to stimuli/ photosynthesis and carbohydrate metabolism
1119	Stem-loop (RNA) binding protein of 41 kDa chloroplastic-like	1.49	1.69	1.31	Response to stimuli/ RNA binding
1910	Ribonucleoprotein; chloroplast; putative	1.36	1.49	2.44	RNA binding
1555	Superoxide dismutase [Fe]	2.99	1.75	1.21	Response to stimuli
1601	Peroxioredoxin	1.8	1.21	1.52	Response to stimuli/ photosynthesis
1655	Peptidyl-prolyl cis-trans isomerase	1.34	1.65	1.59	Response to stimuli/ protein metabolism
1845	Peptidyl-prolyl cis-trans isomerase FKBP12-like	1.37	1.84	1.45	Response to stimuli/ protein metabolism
1867	FKBP-type peptidyl-prolyl cis-trans isomerase	1.43	2.33	1.5	Response to stimuli/ protein metabolism
1540	Proteasome subunit beta type-2-A-like	2.83	2.63	1.31	Protein metabolism
1425	Arginine biosynthesis bifunctional protein ArgJ	1.32	2.59	1.28	Cellular amino acid metabolic process

The average ratio (marked Av ratio) that is statistically significant is marked in bold.

not be assigned to orthologous clusters, other failed to map despite successful assignment. This suggests that KEGG ontology for *S. lycopersicum* may still be incomplete and some clusters are missing. Results of the mapping on selected pathways are shown in **Figure 3** and indicate the carbohydrate and amino acid metabolic pathways were influenced the most by the temperature factor under the three conditions studied: PSV infection, PSV plus satRNA infection, and growth without virus challenge.

DISCUSSION

In plants infected by PSV or PSV plus satRNA, the maximum level of symptoms development was reached earlier for the plants grown at the higher temperature, as observed also for *N. benthamiana* plants infected by the geminiviruses African cassava mosaic virus (ACMV) and Sri Lankan cassava mosaic virus (Chellappan et al., 2005). However, in that study, the



severity of symptoms was greater for plants grown at the lower temperature. Moreover, those authors observed that at higher temperatures newly emerged leaves of the ACMV-infected plants showed recovery from symptom appearance, while this was not the case in our study. In our system, on the day the plants were harvested (21 dpi), the accumulation of viral RNAs and satRNA was higher at the lower temperature, as was confirmed by RT-qPCR, with the exception of the subgenomic RNA encoding the CP, which was higher at 27°C when PSV plus satRNA-infected plants were analyzed. [This is consistent with proteomic data for this condition where larger amounts of CP were found at 27°C than at 21°C; however, differences in PSV CP accumulation in the proteomic part were statistically not significant (not shown).] A similar situation was observed also in the study by Chellappan et al. (2005), where the virus genomic DNA levels were higher at the lower temperature than

at the higher temperature studied, for both geminiviruses. Those authors suggested that the temperature played a major role in decreasing the virus load.

As expected, at the higher temperature, better growth of the plants was observed. The onset of symptom development and their severity were associated with the level of the virus in host cells and clearly suggested major changes in plants metabolism. There are a number of reports on the effect of external abiotic stimuli on plant development, photosynthetic performance and other aspects of primary metabolism (Eastburn et al., 2011; Kosová et al., 2011; Obrepalska-Stęplowska et al., 2013; Wituszyńska et al., 2013; Rodziewicz et al., 2014; Farrant and Ruelland, 2015; George et al., 2015). In the present study, the changes caused by virus infection and temperature could be separated. In addition, the temperature range used was within that supporting the normal growth and not associated with

heat/cold stress. Other studies have examined the effects of infection by pathogenic factors resulting in increases of various elements of the defense machinery including pathogenesis-related proteins (Elvira et al., 2008), heat-shock proteins (Lu et al., 2003; Chen et al., 2008), and RNA silencing (Vance and Vaucheret, 2001; Waterhouse et al., 2001). Zhang et al. (2012) tested other temperature sets for their analysis of interactions of TCV in *Arabidopsis* showing that higher temperature (26°C) facilitated more rigorous replication of this virus than was in the case in plants grown at a lower temperature (18°C). Our results are consistent with this observation.

When mock-inoculated plants grown at the two temperature conditions were compared, the levels of proteins in the categories “protein metabolic process” and “response to stimulus” increased moderately at the higher temperature. The former group represented mostly factors participating in the degradation processes. The increase in peroxiredoxin levels, with a role in oxidative stress control, also was found in another study (Mühlhaus et al., 2011). Proteins in other categories largely decreased moderately. Altogether, it appears that at higher temperature basal plant responses to external stimuli performed better than at 21°C.

The presence of virus is generally known to diminish accumulation of photosynthetic proteins in infected plants (Di Carli et al., 2010; Obrepałska-Stęplowska et al., 2013; Wu et al., 2013; Fang et al., 2015). In this study, this effect was even more intensified in virally-infected plants that were maintained at the higher temperature. This might be the result of not only an increase in temperature but also from an advanced stage of viral infection. Plants respond by production of heat shock proteins to various stresses, and these proteins constitute part of the plant’s adaptive mechanisms for which increased accumulation was observed both at high and low temperature stresses (Timperio et al., 2008). Overall, the results show clearly that the plant response to external factors is more active at the higher temperature, especially when challenged by the virus.

The temperature-dependent induction of plant resistance response to viral infection also was observed previously (Malamy et al., 1992; Baulcombe and Dean, 2014; Prasad and Sonnewald, 2015). The reduced levels of a few proteins might result from their primary role; e.g., in photosynthesis, which seems to perform worse at higher temperature (see below). An increase of proteins functioning in RNA binding was observed and might reflect the reaction to infection by an RNA pathogen (Li and Nagy, 2011). The effectiveness of the plant response was observed among others in *Arabidopsis* challenged by a bacterial pathogen, together with increased level of symptom expression. In that case this plant reaction was thought to be associated with host-pathogen interaction, rather than just an increase in pathogen growth at the higher temperature (Eastburn et al., 2011), which might be also the case in the present study.

SatRNA slightly delayed symptom expression on plants infected with PSV-P at 21°C (Obrepałska-Stęplowska et al., 2013). The presence satRNA in the PSV infection at the higher temperature resulted in fewer differentially-accumulated proteins than for PSV-infected plants, and either did not influence

plant defense proteins, or decreased their level of expression (Obrepałska-Stęplowska et al., 2013).

The most affected proteins in the three studied conditions were those participating in photosynthesis and carbohydrate metabolism. The changes in photosynthetic protein abundance in plants challenged by pathogens is a known phenomenon (Sajani et al., 2007; Garavaglia et al., 2010; Eastburn et al., 2011; Obrepałska-Stęplowska et al., 2013), as this process is among those more sensitive to environmental stressors. Usually, photosynthesis is repressed in response to various types of pathogens (Roberts and Paul, 2006; Major et al., 2010; Kangasjärvi et al., 2012). In mock-inoculated plants and PSV-infected, proteins involved in protein degradation increased in abundance at the higher temperature. Similar responses of proteins responsible for protein degradation also were found in rice leaves exposed to changing temperature (Gammulla et al., 2011). The intense effect on protein metabolism in virus-infected plants can be explained by the necessity to ensure synthesis of various cell compounds, as well as plant-derived metabolites for growth to maintain the cellular integrity of host cells, which is important during early phases of infection by biotrophic and hemibiotrophic pathogens (Kangasjärvi et al., 2012). It might also be of importance for the phase of restoration of metabolism in later stages of infection. Importantly, cellular amino acid metabolic processes also were affected. Most of proteins with this role were higher in abundance. This might be associated with high demands on the host during virus propagation and with cellular recovery of the host after the viral infection has been suppressed. This is significantly less evident in cells infected together by PSV and its satRNA where only one protein spot differentially accumulating at the two temperature conditions was identified. Peptidyl-prolyl-cis trans isomerase is known not only to participate in protein metabolism but also in response to various abiotic stresses including those associated with temperature (Marivet et al., 1994; Gammulla et al., 2011). It seems that in this respect protein metabolism is comparable for plants maintained at the two temperature conditions.

Overall, when all proteomic data for the three examined situations (PSV-infection, PSV plus satRNA-infection and no virus treatment) were compared, it is conceivable that at the higher temperature transport was affected, although not all the differences in the data were statistically significant.

CONCLUSIONS

Summarizing all the data, higher temperature caused a faster growth rate, disease symptom development on plants and initial accumulation of virus, which after reaching a plateau, dropped precipitously. Plants grown at the higher temperature showed a reduction in accumulation of proteins involved in photosynthesis and carbohydrate metabolism as well as transport, and an increase in accumulation of proteins involved in plant response to external stimuli, as well as some involved in protein metabolism. This is especially evident in *N. benthamiana* infected by PSV, where a decrease of proteins involved in the TCA

cycle was observed, and to a lesser extent in mock-inoculated and PSV plus satRNA-infected plants. Additionally, an increase in abundance of proteins involved in amino acid metabolism was observed for PSV-infected plants grown at higher temperature.

ACKNOWLEDGMENTS

This paper was supported by the Polish National Center of Science grant No NN310117537 (to AO). PP is funded by grant no. NRF-2013R1A2A2A01016282 from the

Korean National Research Foundation of the Republic of Korea.

SUPPLEMENTARY MATERIAL

The Supplementary Material for this article can be found online at: <http://journal.frontiersin.org/article/10.3389/fpls.2015.00903>

Supplementary Table S1 | Collective characteristics of identified proteins including their Mascot, Blast2GO, KEGG, and KAAS ortholog definition as well as and KEGG pathway names classified on the basis of *Solanum lycopersicum* database.

REFERENCES

- Altschul, S. F., Madden, T. L., Schäffer, A. A., Zhang, J., Zhang, Z., Miller, W., et al. (1997). Gapped BLAST and PSI-BLAST: a new generation of protein database search programs. *Nucleic Acids Res.* 25, 3389–3402. doi: 10.1093/nar/25.17.3389
- Ashoub, A., Baumlißberger, M., Neupaertl, M., Karas, M., and Brüggemann, W. (2015). Characterization of common and distinctive adjustments of wild barley leaf proteome under drought acclimation, heat stress and their combination. *Plant Mol. Biol.* 87, 459–471. doi: 10.1007/s11103-015-0291-4
- Baulcombe, D. C., and Dean, C. (2014). Epigenetic regulation in plant responses to the environment. *Cold Spring Harb. Perspect. Biol.* 6:a019471. doi: 10.1101/cshperspect.a019471
- Chellappan, P., Vanitharani, R., Ogbe, F., and Fauquet, C. M. (2005). Effect of temperature on geminivirus-induced RNA silencing in plants. *Plant Physiol.* 138, 1828–1841. doi: 10.1104/pp.105.066563
- Chen, Z., Zhou, T., Wu, X., Hong, Y., Fan, Z., and Li, H. (2008). Influence of cytoplasmic heat shock protein 70 on viral infection of *Nicotiana benthamiana*. *Mol. Plant Pathol.* 9, 809–817. doi: 10.1111/j.1364-3703.2008.00505.x
- Conesa, A., and Götz, S. (2008). Blast2GO: a comprehensive suite for functional analysis in plant genomics. *Int. J. Plant Genomics* 2008:619832. doi: 10.1155/2008/619832
- Di Carli, M., Villani, M. E., Bianco, L., Lombardi, R., Perrotta, G., Benvenuto, E., et al. (2010). Proteomic analysis of the plant–virus interaction in Cucumber mosaic virus (CMV) resistant transgenic tomato. *J. Proteome Res.* 9, 5684–5697. doi: 10.1021/pr100487x
- Ding, S.-W., Anderson, B. J., Haase, H. R., and Symons, R. H. (1994). New overlapping gene encoded by the cucumber mosaic virus genome. *Virology* 198, 593–601. doi: 10.1006/viro.1994.1071
- Eastburn, D., McElrone, A., and Bilgin, D. (2011). Influence of atmospheric and climatic change on plant–pathogen interactions. *Plant Pathol.* 60, 54–69. doi: 10.1111/j.1365-3059.2010.02402.x
- Elvira, M. I., Galdeano, M. M., Gilardi, P., García-Luque, I., and Serra, M. T. (2008). Proteomic analysis of pathogenesis-related proteins (PRs) induced by compatible and incompatible interactions of pepper mild mottle virus (PMMoV) in *Capsicum chinense* L3 plants. *J. Exp. Bot.* 59, 1253–1265. doi: 10.1093/jxb/ern032
- Fang, X., Chen, J., Dai, L., Ma, H., Zhang, H., Yang, J., et al. (2015). Proteomic dissection of plant responses to various pathogens. *Proteomics* 15, 1525–1543. doi: 10.1002/pmic.201400384
- Farrant, J. M., and Ruelland, E. (2015). Plant signalling mechanisms in response to the environment. *Environ. Exp. Bot.* 114, 1–3. doi: 10.1016/j.envexpbot.2015.02.006
- Gammulla, C. G., Pascovici, D., Atwell, B. J., and Haynes, P. A. (2011). Differential proteomic response of rice (*Oryza sativa*) leaves exposed to high—and low—temperature stress. *Proteomics* 11, 2839–2850. doi: 10.1002/pmic.201100068
- Garavaglia, B. S., Thomas, L., Gottig, N., Zimaro, T., Garofalo, C. G., Gehring, C., et al. (2010). Shedding light on the role of photosynthesis in pathogen colonization and host defense. *Commun. Integr. Biol.* 3, 382–384. doi: 10.4161/cib.3.4.12029
- George, I. S., Pascovici, D., Mirzaei, M., and Haynes, P. A. (2015). Quantitative proteomic analysis of cabernet sauvignon grape cells exposed to thermal stresses reveals alterations in sugar and phenylpropanoid metabolism. *Proteomics* 15, 3048–3060. doi: 10.1002/pmic.201400541
- Ghoshal, B., and Sanfaçon, H. (2014). Temperature-dependent symptom recovery in *Nicotiana benthamiana* plants infected with tomato ringspot virus is associated with reduced translation of viral RNA2 and requires ARGONAUTE 1. *Virology* 456, 188–197. doi: 10.1016/j.virol.2014.03.026
- Hou, W. N., Duan, C. G., Fang, R.-X., Zhou, X.-Y., and Guo, H.-S. (2011). Satellite RNA reduces expression of the 2b suppressor protein resulting in the attenuation of symptoms caused by Cucumber mosaic virus infection. *Mol. Plant Pathol.* 12, 595–605. doi: 10.1111/j.1364-3703.2010.00696.x
- Kangasjärvi, S., Neukermans, J., Li, S., Aro, E.-M., and Noctor, G. (2012). Photosynthesis, photorespiration, and light signalling in defence responses. *J. Exp. Bot.* 63, 1619–1636. doi: 10.1093/jxb/err402
- Király, L., Hafez, Y. M., Fodor, J., and Király, Z. (2008). Suppression of tobacco mosaic virus-induced hypersensitive-type necrotization in tobacco at high temperature is associated with downregulation of NADPH oxidase and superoxide and stimulation of dehydroascorbate reductase. *J. Gen. Virol.* 89, 799–808. doi: 10.1099/vir.0.83328-0
- Kosová, K., Vítámvás, P., Prášil, I. T., and Renaut, J. (2011). Plant proteome changes under abiotic stress—contribution of proteomics studies to understanding plant stress response. *J. Proteomics* 74, 1301–1322. doi: 10.1016/j.jprot.2011.02.006
- Law, R. D., and Crafts-Brandner, S. J. (2001). High temperature stress increases the expression of wheat leaf ribulose-1, 5-bisphosphate carboxylase/oxygenase activase protein. *Arch. Biochem. Biophys.* 386, 261–267. doi: 10.1006/abbi.2000.2225
- Li, J., Lin, X., Chen, A., Peterson, T., Ma, K., Bertzky, M., et al. (2013). Global priority conservation areas in the face of 21st century climate change. *PLoS ONE* 8:e54839. doi: 10.1371/journal.pone.0054839
- Li, Z., and Nagy, P. D. (2011). Diverse roles of host RNA binding proteins in RNA virus replication. *RNA Biol.* 8, 305–315. doi: 10.4161/rna.8.2.15391
- Lu, J., Du, Z.-X., Kong, J., Chen, L.-N., Qiu, Y.-H., Li, G.-F., et al. (2012). Transcriptome analysis of *Nicotiana tabacum* infected by Cucumber mosaic virus during systemic symptom development. *PLoS ONE* 7:e43447. doi: 10.1371/journal.pone.0043447
- Lu, R., Malcuit, I., Moffett, P., Ruiz, M. T., Peart, J., Wu, A. J., et al. (2003). High throughput virus-induced gene silencing implicates heat shock protein 90 in plant disease resistance. *EMBO J.* 22, 5690–5699. doi: 10.1093/emboj/cdg546
- Major, I. T., Nicole, M.-C., Duplessis, S., and Séguin, A. (2010). Photosynthetic and respiratory changes in leaves of poplar elicited by rust infection. *Photosyn. Res.* 104, 41–48. doi: 10.1007/s11120-009-9507-2
- Malamy, J., Hennig, J., and Klessig, D. F. (1992). Temperature-dependent induction of salicylic acid and its conjugates during the resistance response to tobacco mosaic virus infection. *Plant Cell* 4, 359–366. doi: 10.1105/tpc.4.3.359
- Marivet, J., Margis-Pinheiro, M., Frendo, P., and Burkard, G. (1994). Bean cyclophilin gene expression during plant development and stress conditions. *Plant Mol. Biol.* 26, 1181–1189. doi: 10.1007/BF00040698

- Moriya, Y., Itoh, M., Okuda, S., Yoshizawa, A. C., and Kanehisa, M. (2007). KAAS: an automatic genome annotation and pathway reconstruction server. *Nucleic Acids Res.* 35, W182–W185. doi: 10.1093/nar/gkm321
- Mühlhaus, T., Weiss, J., Hemme, D., Sommer, F., and Schroda, M. (2011). Quantitative shotgun proteomics using a uniform 15N-labeled standard to monitor proteome dynamics in time course experiments reveals new insights into the heat stress response of *Chlamydomonas reinhardtii*. *Mol. Cell. Proteomics* 10:M110.004739. doi: 10.1074/mcp.M110.004739
- Nakasugi, K., Crowhurst, R. N., Bally, J., Wood, C. C., Hellens, R. P., and Waterhouse, P. M. (2013). De novo transcriptome sequence assembly and analysis of RNA silencing genes of *Nicotiana benthamiana*. *PLoS ONE* 8:59534. doi: 10.1371/journal.pone.0059534
- Nersisyan, L., Samsonyan, R., and Arakelyan, A. (2014). CyKEGGParser: tailoring KEGG pathways to fit into systems biology analysis workflows. *F1000Res.* 3:145. doi: 10.12688/f1000research.4410.2
- Netsu, O., Hiratsuka, K., Kuwata, S., Hibi, T., Ugaki, M., and Suzuki, M. (2008). Peanut stunt virus 2b cistron plays a role in viral local and systemic accumulation and virulence in *Nicotiana benthamiana*. *Arch. Virol.* 153, 1731–1735. doi: 10.1007/s00705-008-0166-y
- Obrepalska-Stepłowska, A., Budziszewska, M., and Pospieszny, H. (2008a). Complete nucleotide sequence of a Polish strain of Peanut stunt virus (PSV-P) that is related to but not a typical member of subgroup I. *Acta Biochim. Pol.* 55, 731–739.
- Obrepalska-Stepłowska, A., Budziszewska, M., Wiczorek, P., and Czerwoniec, A. (2012). Analysis of two strains of Peanut stunt virus: satRNA-associated and satRNA free. *Virus Genes* 44, 513–521. doi: 10.1007/s11262-012-0729-6
- Obrepalska-Stepłowska, A., Nowaczyk, K., Budziszewska, M., Czerwoniec, A., and Pospieszny, H. (2008b). The sequence and model structure analysis of three Polish peanut stunt virus strains. *Virus Genes* 36, 221–229. doi: 10.1007/s11262-007-0180-2
- Obrepalska-Stepłowska, A., Wiczorek, P., Budziszewska, M., Jeszke, A., and Renault, J. (2013). How can plant virus satellite RNAs alter the effects of plant virus infection? A study of the changes in the *Nicotiana benthamiana* proteome after infection by Peanut stunt virus in the presence or absence of its satellite RNA. *Proteomics* 13, 2162–2175. doi: 10.1002/pmic.201200056
- Pacheco, R., Garcia-Marcos, A., Manzano, A., de Lacoba, M. G., Camañes, G., García-Agustín, P., et al. (2012). Comparative analysis of transcriptomic and hormonal responses to compatible and incompatible plant-virus interactions that lead to cell death. *Mol. Plant Microbe Interact.* 25, 709–723. doi: 10.1094/MPMI-11-11-0305
- Patil, B. L., and Fauquet, C. M. (2015). Light intensity and temperature affect systemic spread of silencing signal in transient agroinfiltration studies. *Mol. Plant Pathol.* 16, 484–494. doi: 10.1111/mpp.12205
- Pfaffl, M. W., Horgan, G. W., and Dempfle, L. (2002). Relative expression software tool (REST©) for group-wise comparison and statistical analysis of relative expression results in real-time PCR. *Nucleic Acids Res.* 30, e36–e36. doi: 10.1093/nar/30.9.e36
- Pospieszny, H. (1987). Wirus karłowatości orzecha ziemnego (*Peanut stunt virus*)—nowo rozpoznany patogen roślin motylkowatych w Polsce. *Prace Nauk. Inst. Ochr. Roślin* 28, 27–85.
- Prasch, C. M., and Sonnewald, U. (2013). Simultaneous application of heat, drought, and virus to *Arabidopsis* plants reveals significant shifts in signaling networks. *Plant Physiol.* 162, 1849–1866. doi: 10.1104/pp.113.221044
- Prasch, C. M., and Sonnewald, U. (2015). Signaling events in plants: stress factors in combination change the picture. *Environ. Exp. Bot.* 114, 4–14. doi: 10.1016/j.envexpbot.2014.06.020
- Renaut, J., Hausman, J. F., and Wisniewski, M. E. (2006). Proteomics and low-temperature studies: bridging the gap between gene expression and metabolism. *Physiol. Plant.* 126, 97–109. doi: 10.1111/j.1399-3054.2006.00617.x
- Roberts, M. R., and Paul, N. D. (2006). Seduced by the dark side: integrating molecular and ecological perspectives on the influence of light on plant defence against pests and pathogens. *New Phytol.* 170, 677–699. doi: 10.1111/j.1469-8137.2006.01707.x
- Rodziewicz, P., Swarczewicz, B., Chmielewska, K., Wojakowska, A., and Stobiecki, M. (2014). Influence of abiotic stresses on plant proteome and metabolome changes. *Acta Physiol. Plant.* 36, 1–19. doi: 10.1007/s11738-013-1402-y
- Sajmani, C., Zurita, J. L., Roncel, M., Ortega, J. M., Barón, M., and Ducruet, J. M. (2007). Changes in photosynthetic metabolism induced by tobamovirus infection in *Nicotiana benthamiana* studied *in vivo* by thermoluminescence. *New Phytol.* 175, 120–130. doi: 10.1111/j.1469-8137.2007.02074.x
- Schwinghamer, M. W., and Symons, R. H. (1975). Fractionation of cucumber mosaic virus RNA and its translation in a wheat embryo cell-free system. *Virology* 63, 252–262. doi: 10.1016/0042-6822(75)90389-X
- Shen, W. X., Au, P. C., Shi, B. J., Smith, N. A., Dennis, E. S., Guo, H., et al. (2015). Satellite RNAs interfere with the function of viral RNA silencing suppressors. *Front. Plant Sci.* 6:281. doi: 10.3389/fpls.2015.00281
- Suzuki, N., Rivero, R. M., Shulaev, V., Blumwald, E., and Mittler, R. (2014). Abiotic and biotic stress combinations. *New Phytol.* 203, 32–43. doi: 10.1111/nph.12797
- Szittyá, G., Silhavy, D., Molnár, A., Havelda, Z., Lovas, A., Lakatos, L., et al. (2003). Low temperature inhibits RNA silencing-mediated defence by the control of siRNA generation. *EMBO J.* 22, 633–640. doi: 10.1093/emboj/cdg74
- Timperio, A. M., Egidio, M. G., and Zolla, L. (2008). Proteomics applied on plant abiotic stresses: role of heat shock proteins (HSP). *J. Proteomics* 71, 391–411. doi: 10.1016/j.jprot.2008.07.005
- Tuttle, J. R., Idris, A. M., Brown, J. K., Haigler, C. H., and Robertson, D. (2008). Geminivirus-mediated gene silencing from Cotton leaf crumple virus is enhanced by low temperature in cotton. *Plant Physiol.* 148, 41–50. doi: 10.1104/pp.108.123869
- Vance, V., and Vaucheret, H. (2001). RNA silencing in plants—defense and counterdefense. *Science* 292, 2277–2280. doi: 10.1126/science.1061334
- Waterhouse, P. M., Wang, M.-B., and Lough, T. (2001). Gene silencing as an adaptive defence against viruses. *Nature* 411, 834–842. doi: 10.1038/35081168
- Wituszyńska, W., Gałazka, K., Rusaczek, A., Vanderauwera, S., Van Breusegem, F., and Karpiński, S. (2013). Multivariable environmental conditions promote photosynthetic adaptation potential in *Arabidopsis thaliana*. *J. Plant Physiol.* 170, 548–559. doi: 10.1016/j.jplph.2012.11.016
- Wu, L., Han, Z., Wang, S., Wang, X., Sun, A., Zu, X., et al. (2013). Comparative proteomic analysis of the plant–virus interaction in resistant and susceptible ecotypes of maize infected with sugarcane mosaic virus. *J. Proteomics* 89, 124–140. doi: 10.1016/j.jprot.2013.06.005
- Yamori, W., Masumoto, C., Fukayama, H., and Makino, A. (2012). Rubisco activase is a key regulator of non–steady–state photosynthesis at any leaf temperature and, to a lesser extent, of steady–state photosynthesis at high temperature. *Plant J.* 71, 871–880. doi: 10.1111/j.1365-313X.2012.05041.x
- Zhang, X., Zhang, X., Singh, J., Li, D., and Qu, F. (2012). Temperature-dependent survival of Turnip crinkle virus-infected *Arabidopsis* plants relies on an RNA silencing-based defense that requires dcl2, AGO2, and HEN1. *J. Virol.* 86, 6847–6854. doi: 10.1128/JVI.00497-12
- Zhong, S.-H., Liu, J.-Z., Jin, H., Lin, L., Li, Q., Chen, Y., et al. (2013). Warm temperatures induce transgenerational epigenetic release of RNA silencing by inhibiting siRNA biogenesis in *Arabidopsis*. *Proc. Natl. Acad. Sci. U.S.A.* 110, 9171–9176. doi: 10.1073/pnas.1219655110
- Zvereva, A. S., and Pooggin, M. M. (2012). Silencing and innate immunity in plant defense against viral and non-viral pathogens. *Viruses* 4, 2578–2597. doi: 10.3390/v4112578

Conflict of Interest Statement: The authors declare that the research was conducted in the absence of any commercial or financial relationships that could be construed as a potential conflict of interest.

Copyright © 2015 Obrepalska-Stepłowska, Renaut, Planchon, Przybylska, Wiczorek, Barylski and Palukaitis. This is an open-access article distributed under the terms of the Creative Commons Attribution License (CC BY). The use, distribution or reproduction in other forums is permitted, provided the original author(s) or licensor are credited and that the original publication in this journal is cited, in accordance with accepted academic practice. No use, distribution or reproduction is permitted which does not comply with these terms.